Experimental Investigation into the Behaviour of CFS Built-Up Channels Subjected to Axial Compression

Krishanu Roy, Tina Chui Huon Ting, Hieng Ho Lau and James B. P. Lim

Abstract Cold-formed steel (CFS) structural elements are emerging as the preferred solution for many commercial and industrial buildings in the construction industry; thus, the use of built-up CFS channel sections is inevitable. Available design rules, for such back-to-back built-up sections, prescribe modified slenderness approach as mentioned in the AISI and AS/NZS. In the literature, very few results are available for such built-up sections. Sixty experimental tests are reported in this paper, which were conducted on CFS built-up channel sections, connected back-to-back by intermediate fasteners. Tests were conducted for different values of slenderness from short-to-long columns. Results from these built-up column tests are discussed in the context of load–axial shortening relationship, buckling modes and deformed shapes. Experimental results are compared with the AISI and AS/NZS design strengths. Comparison shows that the design strength is approximately 15% more conservative as a whole; however, it overestimates the capacity of built-up columns governed by local buckling failure.

Keyword CFS · Back-to-back channels · Built-up channels · Buckling · Fasteners

Notation

A′   Total web width
A_e Effective cross-sectional area

K. Roy (✉) · J. B. P. Lim
Department of Civil and Environmental Engineering,
University of Auckland, Auckland, New Zealand
e-mail: kroy405@aucklanduni.ac.nz

T. C. H. Ting
Faculty of Engineering and Science, Curtin University Malaysia, Miri, Sarawak, Malaysia

H. H. Lau
Faculty of Engineering, Computing and Science, Swinburne University
of Technology Sarawak Campus, Kuching, Sarawak, Malaysia

B′   Total flange width
C′   Total lip width
t   Section thickness
COV   Coefficient of variation
E Young's modulus
F_n Critical buckling stress
S   Longitudinal spacing between fasteners
λ_c Non-dimensional slenderness ratio

1 Introduction

The increasing needs for innovation to cater for construction needs have led to the development of cold-formed steel (CFS) industry. CFS is very much used due to benefits such as ease of construction, and its high strength to weight ratio, which allows economical and effective design of structural members. One of the innovations is the CFS built-up channels connected back-to-back at the webs (see Fig. 1). It is very effective to use built-up I-section for large span beam and column members. These built-up sections can carry higher loads and can be used for larger spans, e.g. columns in warehouse or shopping malls, steel trusses, portal frames, space frames and wall frames. Current design standards use the modified slenderness approach to estimate the axial capacity of CFS built-up columns based on the design guidelines from the American Iron and Steel Institute [1] and the Australian and New Zealand Standards (AS/NZS 4600:2005) [21]. However, the effectiveness of the modified slenderness approach has not been justified for CFS, unlike hot-rolled steel built-up columns.

Very few literature are available on determining the compressive capacity of CFS built-up channel sections with the configuration in Fig. 1. The authors studied the effect of different fastener spacings in [23], and the influence of thickness in [11] on the capacity of CFS built-up back-to-back channel columns connected at the webs of two channels.

Previous research involves various forms of built-up sections. Piyawat et al. [7] studied on back-to-back built-up columns connected by welds. Zhang and Young [25] researched on CFS built-up columns connected back-to-back with an opening at the web (see Fig. 2). There was also investigation on the axially loaded welded built-up sections connected at the toes done by Whittle and Ramseyer [24]. Other works on back-to-back built-up columns include [2, 5], while CFS built-up columns connected by intermediate screws and wood sheathed were investigated experimentally by Fratamico et al. [6].

Due to limited studies, research on other forms of built-up section serves as important references as well. Dabaon et al. [4] studied on CFS built-up battened columns. They found that the design standards, which include AISI and AS/NZS and the Eurocodes, are un-conservative for columns governed by local buckling failure but are conservative for columns governed by flexural buckling failure. Roy et al. [10,
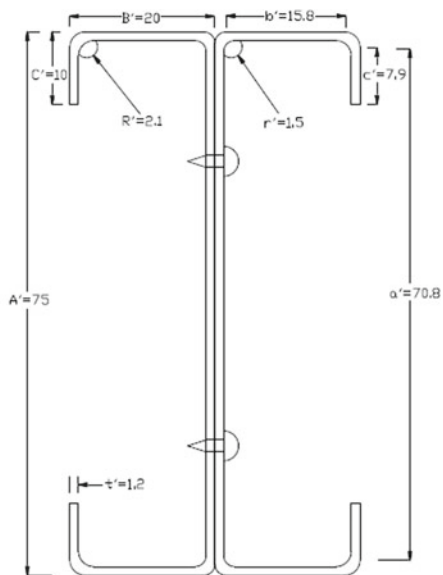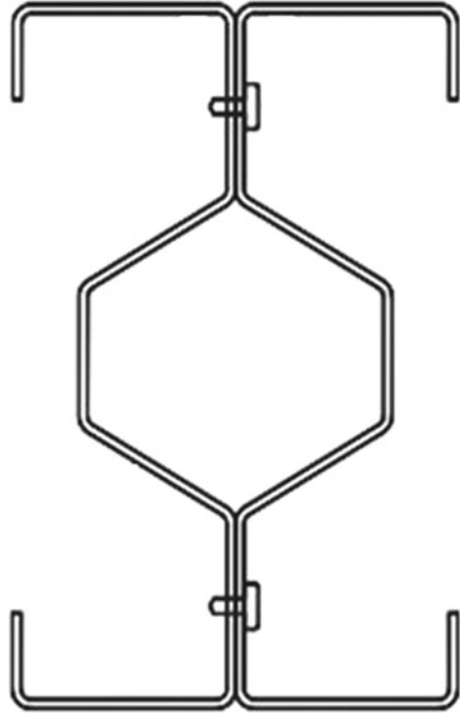
(a) BU75
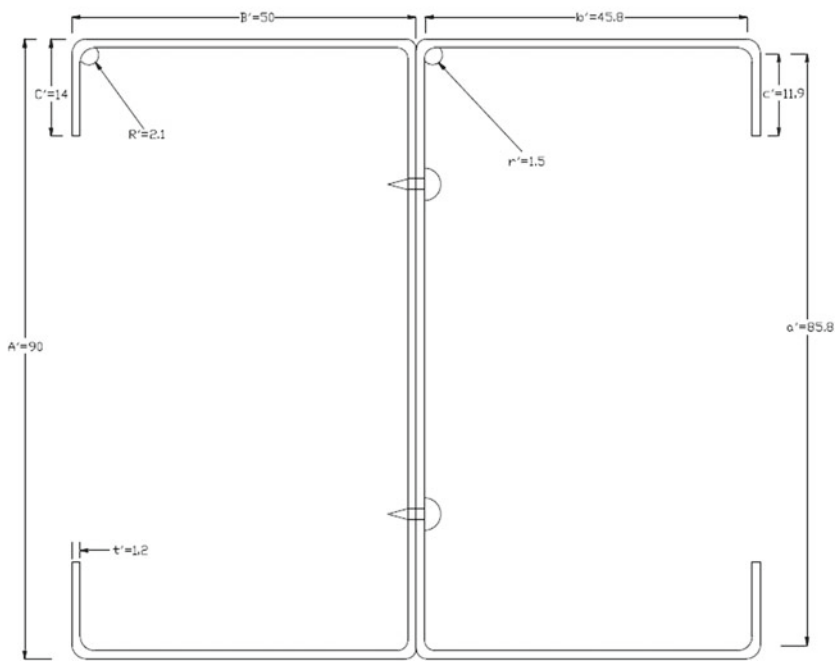
(a) BU90

*Dimensions are in mm

Fig. 1 Dimensions of the investigated CFS built-up channel sections

13, 18] also studied, experimentally and numerically, the axial capacity of back-to-back gapped built-up cold-formed steel-lipped channel sections and concluded that the current design guidelines by AISI and AS/NZS can be too conservative in predicting the axial capacity of such columns. Also, investigated by Roy et al. [12], the behaviour of built-up CFS un-lipped channel sections, connected back-to-back, subjected to compressive force. The cold-formed built-up stainless steel sections under compression were considered by Roy et al. [9, 14, 15, 20]. Axial load capacity of cold-formed steel sections was investigated by Ramseyer [8]. On the other hand, built-up CFS channels connected face-to-face were tested under compression by Roy et al. [16, 17].

This paper presents 60 experimental test results conducted on axially loaded back-to-back built-up CFS channels. Material properties and initial imperfections were determined for all test specimens. The test results are analysed in terms of failure loads, deformed shapes and load–deflection behaviour for two types of cross section, BU75 and BU90, at various lengths of 0.3–2 m. When the experimental strengths were compared against the AISI and AS/NZS, design guidelines are generally safe for columns governed by overall buckling failure, however, are unsafe for built-up channels governed mainly by local buckling failure. A finite element model is presented for these built-up columns by the authors in another paper [19].

2 Current Design Rules as Per AISI and AS/NZS

The theoretical results of the built-up columns investigated were calculated based on the relevant clauses in the American Iron and Steel Institute specifications and the Australia/New Zealand standard. These calculated strengths were later used for comparison with the test strengths. The axial strength for built-up CFS columns is calculated according to the equations from AISI and AS/NZS as follows:

$$P_{AISI} = A_e F_n \tag{1}$$

The critical buckling stress (F_n) is determined as below:

$$\text{For } \lambda_c \leq 1.5 \quad F_n (0.658 \lambda_c^2) F_y \tag{2}$$

$$\text{For } \lambda_c > 1.5 \quad F_n = \left(\frac{0.877}{\lambda_c^2}\right) F_y \tag{3}$$

The non-dimensional critical slenderness (λ_c) is calculated using Eq. 4:

$$\lambda_c = \sqrt{\frac{F_y}{F_e}} \tag{4}$$

Modified slenderness ratio was used for all calculations as per Eq. 5.

$$\left(\frac{KL}{r}\right)_{ms} = \sqrt{\left(\frac{KL}{r}\right)^2 + \left(\frac{s}{r_{yc}}\right)^2}; \quad \text{For which} \left(\frac{s}{r_{yc}}\right) \leq 0.5 \left(\frac{KL}{r}\right)_o \tag{5}$$

3 Experimental Investigations

3.1 Test Specimens

The column specimens consist of channel sections of C75 and C90 as shown in Fig. 1. Built-up column specimen dimension is also shown in Table 1. In total, 60 built-up columns were tested, with four different column heights from 0.3 to 2 m. All the columns were loaded under axial compression and under pin-ended boundary conditions on both ends of the columns, expect the stub column (0.3 m), which was loaded under fixed ended boundary conditions. As shown in Table 1, the following fastener spacings were considered in the test programme.

Table 1 Fastener spacing

Column height (m)	Screw spacing (m)		
	Five locations	Three screw locations	Two screw locations
0.3	0.050	0.100	0.200
0.5	0.100	0.200	0.400
1.0	0.225	0.450	0.900
2.0	0.475	0.950	1.900

Fig. 3 Specimen labelling

Built-up back-to-back channel-sections with nominal 90mm web depth → **BU90**

Nominal fastener spacing 50mm → **S50**

Nominal specimen length → **L300**

Specimen 1 → **-1**
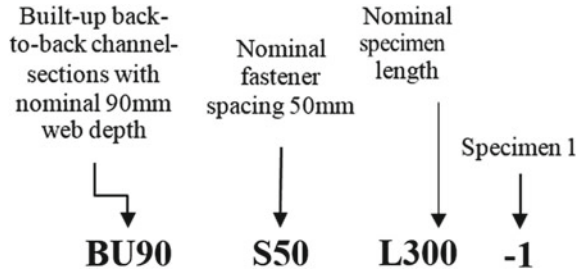
3.2 Determination of Material Properties

The material properties, i.e. the modulus of elasticity and yield stress, were determined using tensile coupon tests in accordance with the British Standard for Testing and Materials [3]. The coupons were cut from both longitudinal and transverse directions with width and gauge length in accordance with the testing standards at 12.5 mm and 50 mm, respectively. A test machine MTS was used to conduct the tensile coupon tests. Load was applied through displacement control. An extensometer of 50 mm gauge length was used to record the strain values. Two strain gauges were also used to measure the strain values. The tensile coupon tests for longitudinal and transverse coupons yield an averaged result of 207 MPa for modulus of elasticity and 560 MPa for yield stress.

3.3 Labelling

Types of the built-up section, fastener spacing, nominal specimen length and test specimen number were coded by the specimen labelling. For example, specimen coding for BU90-S50-L300-1 is shown in Fig. 3. The specimen label shows that the depth of the channel (i.e. the width of the web) is 90 mm as denoted by BU90. BU stands for built-up section. Fastener spacing is denoted by S (50 mm), and the length of the built-up column is 300 mm, as denoted by L. At the end of the label, the number 1 is used to express the specimen number as 1.

3.4 Test Setup and Loading Procedure

All the built-up columns were loaded with the help of a Universal Testing Machine (UTM) (see Fig. 4). The capacity of the UTM was 600 kN. A constant loading rate (below 25 kg/cm^2/s) was maintained during the load application. Six LVDTs were used for short, intermediate and slender built-up column tests, while three LVDTs were used for stub columns. Figure 4 illustrates the locations of the LVDTs, with one LVDT measuring the longitudinal direction for axial shortening, while all other LVDTs measure the transverse direction for lateral displacement of the built-up columns. The failure load was recorded by an external load cell in between the bottom of the specimen and the base plate.

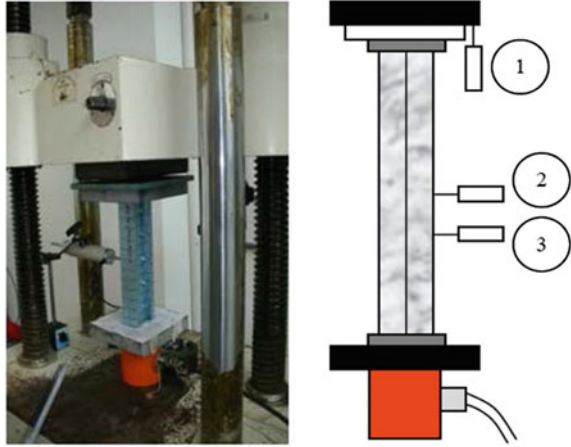## 3.5 Initial Imperfection Measurement

Initial imperfections are caused in cold-formed steel sections because of fabrication error and transportation problem. It is very important to include those geometric imperfections in finite element models to validate the results of experimental tests. An imperfection measurement setup is shown in Fig. 5a. The imperfection measurement was conducted on all test specimens using an LVDT of 0.001 mm precision at an interval of 20 mm. LVDT positions for imperfection measurements are shown in Fig. 5b. In Fig. 5c, initial imperfections are plotted against the length of the built-up columns for BU90S200L300-1. It was found that the maximum imperfections for the test specimens were 0.2 mm for 0.3 m specimen, 0.2 mm for 0.5 m specimen, 0.4 mm for 1 m specimen and 0.6 mm for 2 m specimen. These values can be used as imperfections input for the finite element models to yield a better axial capacity prediction for the test specimens [16].

3.6 Results from Experimental Tests

Table 2 summarises the dimensions of the built-up specimens tested and the respective experimental failure loads (P$_{EXP}$). In order to compare the experimental results to the design strength, AISI and AS/NZS strengths are also included in Table 2a for BU75 and Table 2b for BU90. The modified slenderness's of all test specimens are calculated and shown in Table 2. Comparison of design and test strengths shows that columns governed by global buckling failure are conservatively predicted by the design standard; however, columns governed by local buckling failure (i.e. stub columns) are un-conservatively predicted by the design standard.

Graph of load versus axial shortening for BU75S50L300-1 is shown in Fig. 6. The graph shows a linear relationship between the load and axial shortening up to 70% (85 kN) of the failure load (120.7 kN) for BU75S50L300-1. Plastic behaviour

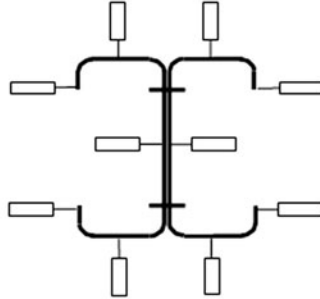**Fig. 4** Built-up column test setup

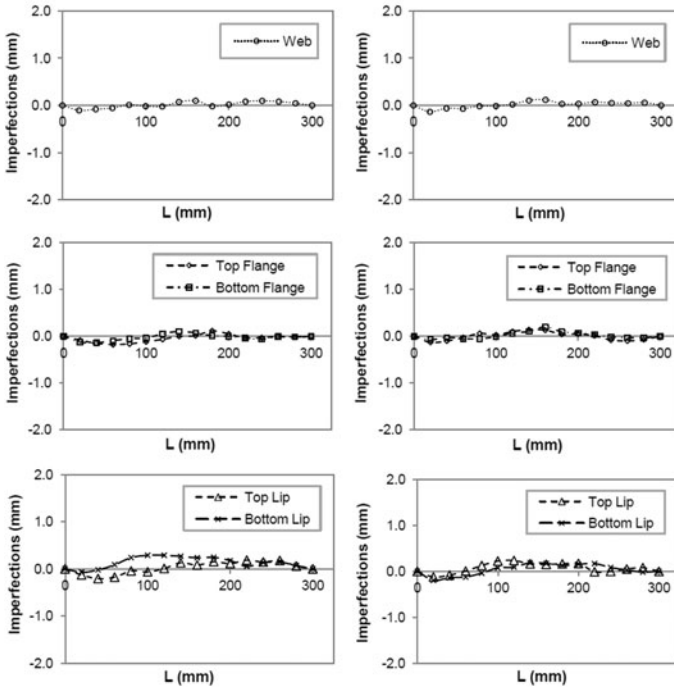

(a) 0.3 m high built-up column test
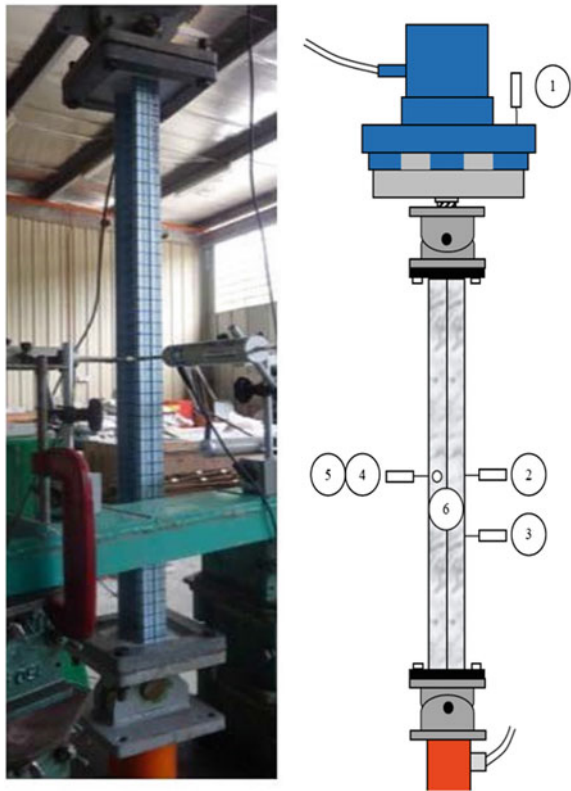
(b) 1 m high built-up column test

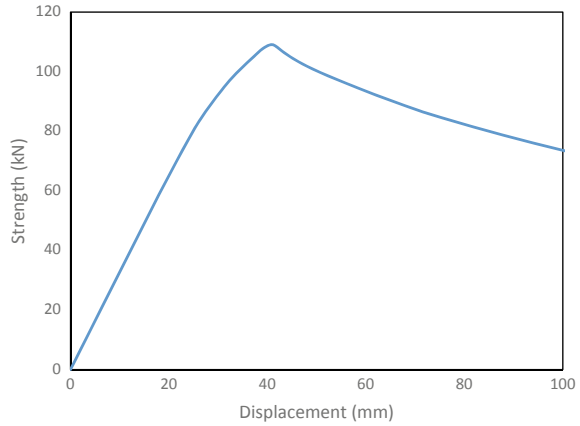(a) Photo of the imperfection measurement setup

(b) Position of LVDTs for imperfection measurement

(c) Initial imperfections for BU90-S200-L300-1

Fig. 5 Details of imperfection measurements

Fig. 6 Typical experimental test results for stub column of BU 75 series with five screws

was observed for BU75S50L300-1, when the load was increased beyond 85 kN and the non-linear behaviour continued up to the failure.

It was observed that at different slenderness, the columns are governed by different failure modes. It was also noticed that the behaviour of the built-up columns is significantly influenced by the change in screw spacing except for stub columns. The stub columns from both BU75 and BU90 were governed by local buckling failure. This happens even when the screw spacing was decreased from 5 to 3. No distortional buckling was observed. Although two channels in a built-up section buckled separately between the screws (see Fig. 7a), both BU75S200L300 and BU90S200L300

Table 2 Experimental test results

Specimen	Web	Flange	Lip	Length	Thickness	Spacing	Modified slenderness	Test results	AISI and AS/NZS design strengths	
	A′	B′	C′	L	t	S	$(KL/r)_m$	P_{EXP}	P_{AISI}	P_{Exp}/P_{AISI}
	(mm)	(mm)	(mm)	(mm)	(mm)	(mm)	–	(kN)	(kN)	–
(a) BU75										
Stub										
BU75S50L300-1	73.1	19.8	11.1	273.0	1.20	50.0	15.63	120.7	126.68	0.95
BU75S50L300-2	73.1	19.8	11.2	280.1	1.21	50.0	15.93	118.8	126.77	0.94
BU75S50L300-3	72.7	19.5	10.8	270.0	1.20	50.9	15.92	118.7	124.84	0.95
BU75S100L300-2	73.1	19.8	11.2	267.2	1.18	99.7	19.48	117.5	125.1	0.94
BU75S100L300-3	73.1	19.9	11.2	273.0	1.19	100.2	19.41	122.7	125.41	0.98
BU75S100L300-4	73.6	19.7	11.2	273.3	1.20	99.5	19.56	115.4	124.89	0.92
BU75S200L300-1	73.7	19.8	11.2	266.4	1.21	200.0	30.31	122.5	119.05	1.03
BU75S200L300-2	73.6	19.9	11.2	266.5	1.20	199.5	30.22	119.1	119.09	1.00
BU75S200L300-3	72.9	20.0	11.2	268.4	1.20	200.0	29.97	113.1	119.36	0.95
Mean										0.96
COV										0.04

(continued)

Table 2 (continued)

Specimen	Web	Flange	Lip	Length	Thickness	Spacing	Modified slenderness	Test results	AISI and AS/NZS design strengths	
	A'	B'	C'	L	t	S	$(KL/r)_m$	P_{EXP}	P_{AISI}	P_{Exp}/P_{AISI}
	(mm)	(mm)	(mm)	(mm)	(mm)	(mm)	–	(kN)	(kN)	–
Short										
BU75S100L500-1	73.6	19.8	11.2	655.0	1.20	100.0	69.11	83.0	78.881	1.05
BU75S100L500-3	73.6	19.7	11.2	680.0	1.21	100.5	72.16	74.1	78.376	0.95
BU75S200L500-1	73.5	19.5	11.3	653.0	1.20	195.0	73.36	86.2	79.992	1.08
BU75S200L500-2	73.6	19.6	11.3	678.0	1.18	195.0	75.58	88.9	81.406	1.09
BU75S200L500-3	73.4	19.7	11.3	680.0	1.19	200.5	75.61	93.6	86.759	1.08
BU75S400L500-1	73.6	19.7	11.3	678.0	1.20	400.0	88.74	74.8	72.417	1.03
BU75S400L500-2	73.5	19.7	11.3	679.0	1.22	401.0	89.00	80.6	74.336	1.08
Mean										1.05
COV										0.05
Intermediate										
BU75S225L1000-1	75.3	20.2	10.4	1133.1	1.20	225.3	121.36	47.0	42.34	1.11
BU75S225L1000-2	75.7	19.9	10.4	1131.2	1.20	225.3	123.71	46.3	41.05	1.13
BU75S450L1000-1	75.8	19.9	10.4	1131.6	1.21	447.0	133.91	50.4	38.98	1.29
BU75S450L1000-2	75.6	19.9	10.4	1133.4	1.20	450.0	135.07	45.0	38.12	1.18
BU75S450L1000-3	75.9	19.8	10.3	1182.2	1.18	450.0	140.52	41.8	34.62	1.21
BU75S900L1000-1	76	19.9	10.3	1131.3	1.19	900.0	171.43	39.9	33.21	1.20
BU75S900L1000-2	76.3	19.8	9.1	1133.4	1.20	900.0	178.06	33.7	30.29	1.11
BU75S900L1000-3	75.9	19.8	10.3	1183.3	1.22	901.0	176.55	31.5	28.91	1.09
Mean										1.17
COV										0.07
Slender										
BU75S475L2000-2	73.9	20.3	10.7	2184.4	1.20	474.5	231.20	10.9	10.27	1.03
BU75S475L2000-3	73.6	20.2	10.8	2183.6	1.20	462	231.61	10.8	10.22	1.03
BU75S950L2000-2	73.5	20.3	10.8	2184.2	1.18	949.5	255.17	8.8	8.43	1.02
BU75S950L2000-3	73.4	20.2	10.8	2184.4	1.17	950.0	256.21	8.6	8.36	1.01
BU75S1900L2000-2	73.1	20.3	10.9	2183.2	1.18	1900.0	334.82	7.6	7.34	1.03
BU75S1900L2000-3	73.7	20.4	10.7	2184.2	1.19	1901.0	333.86	7.5	7.31	1.01
Mean										1.02
COV										0.01
(b) BU90										
Stub										
BU90S50L300-1	91.3	49.8	14.6	277.0	1.20	50.0	7.95	172.5	179.7	0.96
BU90S50L300-2	91.8	49.7	14.5	272.0	1.19	49.8	7.89	171.6	182.6	0.94
BU90S50L300-3	92.9	49.4	14.5	261.0	1.21	50.0	7.93	170.6	179.6	0.95
BU90S100L300-1	90.8	49.7	14.6	262.0	1.20	99.9	9.45	166.2	178.7	0.93
BU90S100L300-2	90.6	49.5	14.6	268.0	1.18	100.0	9.42	165.8	176.4	0.94
BU90S200L300-1	90.7	49.4	14.6	273.5	1.18	201.0	11.93	163.3	175.6	0.93

Table 2 (continued)

| Specimen	Web	Flange	Lip	Length	Thickness	Spacing	Modified slenderness	Test results	AISI and AS/NZS design strengths	
	A'	B'	C'	L	t	S	$(KL/r)_m$	P_{EXP}	P_{AISI}	P_{Exp}/P_{AISI}
	(mm)	(mm)	(mm)	(mm)	(mm)	(mm)	–	(kN)	(kN)	–
BU90S200L300-2	90.7	49.4	14.6	269.5	1.20	199.0	11.83	163.5	173.9	0.94
BU90S200L300-3	89.5	48.3	14	280.5	1.20	199.0	11.87	162.9	173.3	0.94
BU90S50L300-1	91.3	49.8	14.6	277.0	1.20	50.0	7.95	172.5	179.7	0.96
Mean										0.94
COV										0.01
Short										
BU90S100L500-1	90.6	49.5	14.6	656	1.21	100.5	35.42	160.4	149.9	1.04
BU90S100L500-2	90.6	49.4	14.6	678	1.20	100.5	34.25	158.1	152.0	1.08
BU90S200L500-1	90.4	49.3	14.7	653	1.18	199.5	38.52	152.2	140.9	1.09
BU90S200L500-2	90.4	49.3	14.7	678	1.19	199.5	39.41	150.9	138.4	1.10
BU90S200L500-3	90.4	49.3	14.6	680	1.21	200.5	40.20	149.2	135.6	1.06
BU90S400L500-1	90.6	49.4	14.7	678	1.18	400.0	50.20	132.4	124.9	1.06
BU90S400L500-2	90.4	49.4	14.7	678	1.20	399.0	49.41	134.5	126.9	1.07
Mean										1.07
COV										0.02
Intermediate										
BU90S225L1000-1	90.8	49.6	14.4	1182	1.21	225.0	60.42	102.6	92.43	1.11
BU90S225L1000-2	90.6	49.6	14.3	1132	1.20	225.0	58.21	102.0	92.72	1.10
BU90S450L1000-1	90.6	49.7	14.4	1130	1.21	450.0	64.21	96.51	86.18	1.12
BU90S450L1000-2	90.4	49.7	14.4	1182	1.18	448.0	66.21	94.42	82.79	1.14
BU90S450L1000-3	90.5	49.8	14.5	1180	1.19	452.0	65.29	93.33	82.54	1.13
BU90S900L1000-1	90.5	49.6	14.4	1131	1.20	897.0	75.21	89.55	82.89	1.08
BU90S900L1000-2	91.0	49.3	14.4	1182	1.21	899.0	77.21	87.58	80.31	1.09
BU90S900L1000-3	90.1	49.2	14.5	1129	1.22	896.0	76.50	87.51	79.51	1.10
Mean										1.11
COV										0.07
Slender										
BU90S475L2000-1	90.6	49.5	14.5	2164	1.20	474.2	92.52	65.4	61.12	1.07
BU90S475L2000-2	90.7	49.4	14.3	2172	1.20	466.6	94.42	66.01	61.63	1.07
BU90S950L2000-1	90.5	49.5	14.6	2169	1.18	960.4	101.17	54.02	50.90	1.06
BU90S950L2000-2	90.4	49.2	14.5	2148	1.17	949.3	103.21	45.62	43.41	1.05
BU90S1900L2000-1	90.5	49.3	14.6	2158	1.18	1902.4	115.20	48.04	44.8	1.07
BU90S1900L2000-2	90.9	49.7	14.2	2152	1.19	1906.7	116.42	43.21	41.14	1.05
Mean										1.06
COV										0.02

test specimens had two fasteners each. Due to less number of fasteners, the back-to-back channels pry apart at the mid-height of the built-up column. For short column of BU75 series, local buckling was the pre-dominant mode of failure at the start of the test; however, at the end of test global bucking was observed for BU75 columns having two fasteners (see Fig. 7b). For intermediate columns of both test series, mostly overall buckling was seen (see Fig. 7c). However, some columns of BU90-L1000 failed through flexural–torsional buckling. Most of the slender columns were dominated by overall buckling failure, showing a large lateral deformation at the middle of the columns (see Fig. 7d). Some failure modes of slender columns of BU90 series were governed by local–global buckling interactions. Once the columns reached failure load, the built-up specimens showed local deformation on the compression side at the mid-height.

4   Comparison with Design Standards

The experimental and theoretical results for BU75 and BU90 are tabulated in Table 2(a) and 2(b), respectively. The theoretical results are calculated using the design steps documented in AISI and AS/NZS, which involves the modified slenderness approach. Comparison of the experimental and theoretical results shows that the design standard is on average 12% more conservative in predicting the capacity of columns governed by overall buckling failure; however, prediction for stub columns governed by local buckling failure was approximately 10% un-conservative.

Table 2a, b also shows that the influence of fastener spacing is negligible in stub and slender columns; however, the effect is significant for short and intermediate columns. Fastener spacing is influential on slender columns because the test specimens failed in global buckling. For short and intermediate columns, the increment of twice the screw spacing reduced the axial strength by approximately 5–10% and 10–15%, respectively.

Graph of design strength versus modified slenderness ratio was plotted on BU75 in Fig. 8a and BU90 on Fig. 8b. Figure 8a shows that at modified slenderness ratio of less than 32, local buckling failure is dominant, while, at modified slenderness ratio of greater than 53, global buckling failure is dominant. Similar trend is observed in the BU90 series in Fig. 8b. Local buckling failure was noticed when the modified slenderness is less than 29, and global buckling failure was observed when the modified slenderness ratio was greater than 48. The behaviour of the slender columns was as anticipated, whereby there was minimal increase in axial strength when the number of screws increases. Generally, the design standards are conservative when overall buckling governed the failure mode of the columns but un-conservative by approximately 10% when local buckling dominated the column's failure mode.
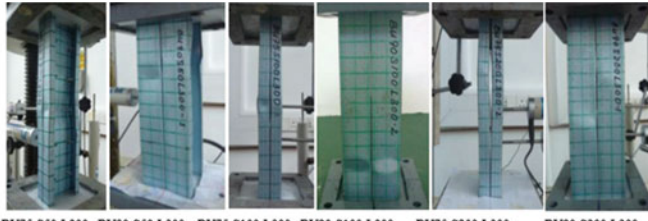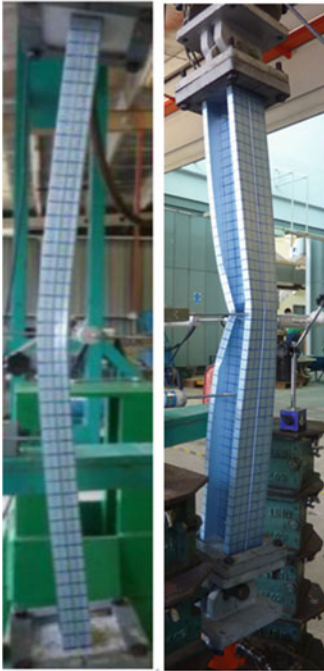
BU75-S50-L300 BU90-S50-L300 BU75-S100-L300 BU90-S100-L300 BU75-S200-L300 BU90-S200-L300
(a) Stub column

BU75-S200-L500   BU90-S200-L500
(b) Short column

BU75-S225-L1000   BU90-S225-L1000   BU75-S950-L2000   BU90-S950-L2000
(c) Intermediate column   (d) Slender column

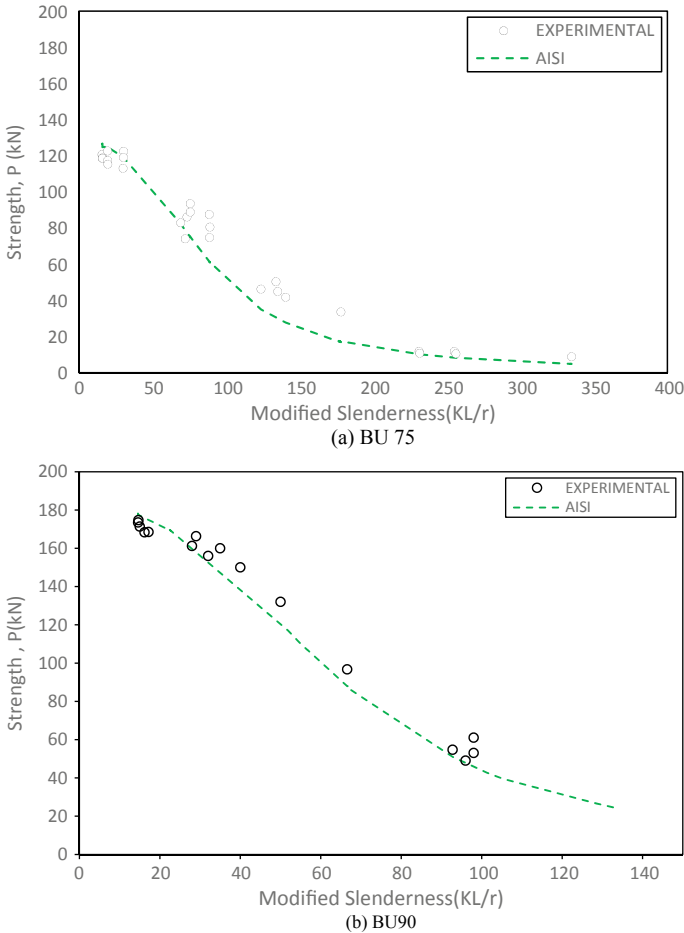**Fig. 7**   Built-up columns at failure

(a) BU 75

(b) BU90

Fig. 8 Plot of axial strength against the modified slenderness

5 Conclusions

This paper presented a total of 60 experimental tests on axially loaded back-to-back built-up CFS channel sections for investigation. The material properties and geometric imperfections for all specimens were measured. Two cross sections, BU75 and BU90, at varying lengths from 0.3 to 2 m were involved in the investigation. The failure modes and load carrying capacities at failure were compared and analysed. Comparison of test results and design strength from AISI and AS/NZS shows that the column capacity predicted by the design standards is conservative for specimens with overall buckling failure but un-conservative for specimens with local buckling failure.

Ongoing work will aim to develop better design methods, for different types of CFS built-up columns, with improved approximations of the column cross sections and end conditions. The authors are following this work to further develop a numerical model to study the different parameters affecting the strength of back-to-back built-up CFS columns including explicit modelling of web fasteners.

References

1. American Iron and Steel Institute (2012) North American specification for the design of cold-formed steel structural members, NAS S100
2. Anbarasu M, Bharath KP, Sukumar S (2014) Study on the capacity of cold-formes steel built-up battened colums under axial compression. Latin Am J Solids Struct 11(12):1375–2271
3. BS EN (2001) Tensile testing of metallic materials method of test at ambient temperature, British Standards Institution
4. Dabaon M, Ellobody E, Ramzy K (2015) Nonlinear behavior of built-up cold-formed steel section battened columns. J Constr Steel Res 110:16–28
5. Fratamico DC, Schafer BW (2014) Numerical studies on the composite action and buckling behavior of built-up cold-formed steel columns. In: 22nd international specialty conference on cold-formed steel structures, St. Louis, MO
6. Fratamico DC, Torabian S, Rasmussen KJR, Schafer BW (2016) Experimental studies on the composite action in wood-sheathed and screw-fastened built-up cold-formed steel columns. In: Proceedings of the annual stability conference structural stability research council, Orlando, FL
7. Piyawat K, Ramseyer C, Kang Thomas H-K (2013) Development of an axial load capacity equation for doubly symmetric built-up cold-formed sections. J Struct Eng Am Soc Civil Eng 139(12):04013008–13
8. Ramseyer CCE (2006) Axial load capacity of cold-formed steel sections, PhD dissertation, University of Oklahoma, Norman, USA
9. Roy K, Lim JBP (2018) Numerical investigation into the buckling behaviour of face-to-face built-up cold-formed stainless steel channel sections under axial compression. Structures (revised)
10. Roy K, Ting TCH, Lau HH, Lim JB (2018) Nonlinear behaviour of back-to-back gapped built-up cold-formed steel channel sections under compression. J Constr Steel Res 147:257–276
11. Roy K, Ting TCH, Lau HH, Lim JB (2018) Effect of thickness on the behaviour of axially loaded back-to-back cold-formed steel built-up channel sections—experimental and numerical investigation. Structures 16:327–346
12. Roy K, Ting TCH, Lau HH, Lim JB (2018) Nonlinear behavior of axially loaded back-to-back built-up cold-formed steel un-lipped channel sections. Steel Compos Struct Int J 28(2):233–250
13. Roy K, Ting TCH, Lau HH, Lim JBP (2018) Compression tests on back-to-back gapped built-upcold-formed steel channel sections. In: Proceedings of the international conference on engineering research and practice for steel construction 2018 (ICSC 2018), Hong Kong, China
14. Roy K, Lau HH, Lim JBP (2018) Finite element modelling of back-to-back built-up cold-formed stainless-steel lipped channels under axial compression. Steel Compos Struct Int J, under review
15. Roy K, Ting TCH, Lau HH, Lim JBP (2018) Effect of screw spacing into the behaviour of back-to-back cold-formed duplex stainless steel built-up channel sections under compression. In: Proceedings of the international conference on engineering research and practice for steel construction 2018 (ICSC 2018), Hong Kong, China
16. Roy K, Mohammadjani C, Lim JB (2018) Experimental and numerical investigation into the behaviour of face-to-face built-up cold-formed steel channel sections under compression. Thin-Walled Struct 134:291–309

17. Roy K, Ting TCH, Lau HH, Lim JBP (2018) Experimental and numerical investigations on axial capacity of CFS built-up box sections. J Constr Steel Res (revised)
18. Roy K, Ting TCH, Lau HH, Lim JBP (2018) Experimental investigation into the behaviour of back-to-back gapped built-up cold-formed steel channel sections under compression. In: Wei-Wen Yu international specialty conference on cold-formed steel structures 2018, 7–8 November, 2018, St. Louis, Missouri, USA
19. Roy K, Ting TCH, Lau HH, Lim JBP (2018) Finite element modelling of built-up CFS channel columns under axial load. In: International conference on the 'Trends and recent advances in civil engineering-TRACE-2018', 23rd to 24th August, 2018, Noida, Uttar Pradesh, India
20. Roy K, Lau HH, Lim JBP (2019) Numerical investigations on the axial capacity of back-to-back gapped built-up cold-formed stainless steel channels. Adv Struct Eng (revised)
21. Standards Australia (2005) Cold-formed steel structures, AS/NZS 4600:2005, Standards Australia/ Standards New Zealand
22. Stone TA, LaBoube RA (2005) Behaviour of cold-formed steel built-up I-sections. Thin-Walled Struct 43(12):1805–1817
23. Ting TCH, Roy K, Lau HH, Lim JBP (2018) Effect of screw spacing on behavior of axially loaded back-to-back cold-formed steel built-up channel sections. Adv Struct Eng 21(3):474–487
24. Whittle J, Ramseyer C (2009) Buckling capacities of axially loaded, cold-formed, built-up channels. Thin-walled Struct 47(2):190–201
25. Zhang JH, Young B (2012) Compression tests of cold-formed steel I-shaped open sections with edge and web stiffeners. Thin-Walled Struct 52:1–11